Hybrid multiscale simulation reveals focusing of a diffusing

peptide molecule by parallel shear flow in water

J. Hu, [1] *I.A. Korotkin,* [1] *S.A. Karabasov* [1]

[1]*The School of Engineering and Materials Science, Queen Mary University of London, Mile End Road, E1 4NS*

London, United Kingdom

Abstract

The hybrid Molecular Dynamics - Fluctuating Hydrodynamics model is extended for multi-resolution simulations of molecular diffusion in water under a steady shear flow. Cases of water self-diffusion and a small protein diffusion in water are considered. For the switched-off flow effect, the model is validated in comparison with the reference all-atom equilibrium molecular dynamics solution. With the flow effect included, the multiscale model correctly captures the meanflow velocity distribution as well as the difference between mean square deviations in different directions with respect to the flow in accordance with the diffusion theory. Results of the simulations are analysed in the context of using hydrodynamic flow gradients for molecular diffusion focusing.

Key words: multi-scale modelling, molecular dynamics, two-phase flow analogy, soft matter, Couette flow, diffusion

1. Introduction

In the past few decades, Microfluidic (MF) technology has become a research topic of increasing interest, as it can be used for a wide range of practical applications, such as

biomaterial synthesis. In comparison with traditional bench-scale systems, microfluidic devices are advantageous because of their low fabrication costs, less material and reagent consumption, improved performance, reduced measurement time, and higher analysis speed [1], [2]. The well-established manufacture of MF devices offers an opportunity for optimisation of complicated channel designs [3], [4] with reproducing specific flow characteristics and accurate timing between different phases of material synthesis [5]. For example, MFs are useful for the study of biofilms because of their ability to precisely adjust the wall shear stress, chemical gradients and the temperature. One important application of MFs is in microfabrication of liquid interfaces created by two-fluid laminar flow in microfluidic channels where controlled chemical reactions can be implemented [6], [7]. The shear flow gradient created under low Reynolds number flows are also extensively used in biotechnology [8], microreactors [9], biological membrane fabrication [10], as well as in chemical separation, extraction and detection [11]–[14].

In most two-fluid laminar flow devices, there is a dense working fluid used such as water at normal conditions, the operational flow speed is low, and the geometric size of the flow device is macroscopic. These make flows in such devices amenable to continuum mechanics of incompressible flows. Computational methods for solving incompressible Navier-Stokes equations, such as the pressure correction method by Chorin [15], exist since the 1960s. At the same time, it is well-known that continuum mechanics models break down in cases where a characteristic dimension of the investigated system reaches nanoscale as in the case of flow inside a nanotube [16]. The same is also the case in dual-stream laminar-flow modelling if in addition to the bulk flow modelling it is also required to resolve chemical reactions at the interface between the two streams. If both the hydrodynamic flow and the internal liquid structure together with constitutive properties of the liquid interface are to be simulated in a micro-fluidic device, a multi-resolution method has to be used.

Not surprisingly, multi-resolution modelling of liquids under parallel shear flow conditions, the so-called Couette flow, has been a popular benchmark case in the multiscale modelling literature. The Couette flow can be readily realised in the experiment by considering a viscous fluid contained in a small channel where one of the parallel walls is moved so that it slides at a constant distance with respect to the other wall. The analytical solution in continuum mechanics either for the start-up or the steady Couette flow is also easy to establish since the governing incompressible Navier-Stokes equations reduce to a one-dimensional diffusion problem in this case. At the scale of discrete molecules, the problem becomes hardly amenable to analytical modelling. Hence, both the start-up and the steady Couette problem have been in the focus of investigation of hybrid molecular dynamics (MD) - continuum mechanics models.

The simulation domain typically contains both the fluidic and the solid wall part of the problem where one wall is stationary and the other one is moving. For simplicity, in many cases the interface between the MD and continuum mechanics part is aligned with the plane of the walls, which allows treating one of the walls at a fully atomistic resolution and simulate the effect of the other wall with continuum mechanics.

In the literature, there are various strategies used to connect the MD particle and the continuum fluid dynamics description of the liquid contained by the walls. For example, in the MD-continuum mechanics model [17], [18], a finite overlap region is utilised for coupling state solution variables of the two representations with achieving a good consistency of the mean-flow velocity profile on both sides of the interface zone with the analytical solution. The same meanflow solution consistency is achieved by [19] who used a flux coupling scheme to connect mass and momentum fluxes of the continuum and atomistic representations on the opposite sides of the interface. Alternatively, as it was shown by [20], one can use the point-wise coupling (PWC) hybrid approach for the same computational

domain decomposition between the continuum and the MD parts of the solution. The latter implementation also probed the solution sensitivity of hybrid approaches to factors like the width of the molecular dynamics domain, the channel height, and the wall roughness. Sensitivity of the Couette flow solution to the parameters of MD-continuum mechanics coupling was also tested by [21], who combined two open-source solvers in the hybrid model, LAMMPS for the MD computation and OpenFOAM for the continuum flow modelling. In the study, both the effect of the solid wall density and the solid-liquid interaction on the non-slip boundary condition of the Couette flow problem are investigated. Under a suitable calibration of the model parameters, it is shown that the solution of such hybrid model for the velocity distribution profile can be in a good agreement with the analytical solution regardless of whether the moving wall boundary condition is applied on the continuum or the atomistic side of the computational domain.

Hybrid all-atom molecular dynamics − continuum mechanics schemes are not the only example of multiscale methods which have been tested on the Couette problem. From the class of multi-resolution MD particle schemes, Smooth Dissipative Particle Dynamics (SDPD) has been applied by [22] to test accuracy of the SDPD model over a range of particle scales for the same Couette problem. In comparison with the MD-continuum mechanics studies, the no-slip boundary correction applied on the walls of the SDPD model was imposed with an adaptive shear correction. In such implementation, one of the walls corresponds to a fine particle resolution, the other wall corresponds to a coarse resolution, and the two representations are connected through the hybrid interface of a finite thickness that is aligned with the walls. Again, the consistency of the multiscale model was demonstrated by a good agreement of its locally averaged hydrodynamic solution field with the analytical meanflow velocity solution in both the coarse and the fine resolution parts of the simulation domain.

The Couette problem has also been used as a test bed for further sophisticated hybrid multi-resolution models, such as the ones which combine an all-atom MD, a mesoscale particle model, and a continuum hydrodynamics description. For example, a triple-decker algorithm that couples the MD, DPD and the Navier-Stokes equations was developed by [23]. In this model, the top wall, which moves at a constant velocity, is a part of the continuum hydrodynamics solution. The interfaces between the continuum hydrodynamics and the mesoscale (DPD) particle zone and between the DPD zone and the MD part are aligned with the flow. A two-layer DPD/MD version of the same triple deck model was also tested. To simulate the non-slip boundary condition, a combination of numerical pressure force, specular reflection and adaptive shear force, which depends on the distance of the particle to the boundary, is used. On the hybrid interface, an adaptive shear forcing is applied to prevent the "phase separation". It was shown that, for an appropriate calibration of the model parameters with and without a finite overlap between the different zones, a good agreement with the analytical meanflow velocity solution is obtained. Another example of a "triple-decker" scheme application for the Couette flow problem can be found in [24] where the SDPD model by [22] was combined with the AdResS method [25] to obtain a compound multi-resolution SDPD-MD algorithm. In comparison with other hybrid simulations of the Couette problem, the mentioned model not only considered the case where the hybrid interfaces between the MD and coarse-grained representations of liquid are parallel to the walls but also when the hybrid interface is normal to the wall plane. The model performance under various combinations of the calibration parameters is tested. In each case, a good agreement with the reference analytical solution for the meanflow velocity profile is demonstrated. A further example of "triple-decker" algorithms can be found in [26], which also uses the AdResS interface to combine MD and DPD in order to bridge the micro- and

mesoscopic descriptions. For a smooth supramolecular coupling in hybrid simulations of water at ambient conditions, that work uses a molecule clustering algorithm.

Despite the abundance of hybrid multiscale methods, which have been tested on the Couette flow problem, the number of publications where multi-resolution modelling has been applied to study the transport properties of complex inhomogeneous fluids beyond the idealised cases of argon or pure water is much less. For example, in addition to the existing publications which are focused on the diffusion and visco-elastic properties of homogenous polymer melts under velocity strain conditions [27]–[30], the only other publication known to the authors where a multi-resolution method has been applied for a composite fluid under flow is [31]. However, the focus of the latter simulation was to compute the Stokes drag exerted on a golf-ball-shape buckyball particle (C540 fullerene) under the effect of a uniform flow field, where the nanoparticle displacement due to flow effects was neglected.

On the other hand, multi-scale modelling of complex heterogeneous fluids such as a biomolecule diffusion in water under shear flow conditions would be of direct relevance to the design of microfluidic devices. For example, it can be expected that molecular diffusion properties at the interface between the two flow streams of dual-stream flow devices are different in comparison with molecular diffusion away from the interface since the velocity strain affects diffusion speed especially for anisotropic and non-Newtonian fluids [32], [33]. Hence, scale-resolved modelling of molecular diffusion under shear conditions is in the focus of the current publication.

In molecular dynamics simulations, there are two popular methods to calculate the molecular diffusion coefficient. One method is based on the non-equilibrium molecular dynamics (NEMD) simulations [34]–[36], [37], where an explicit forcing is applied to the solid wall

atoms, which generates drag on the fluid in the Couette problem. The second method is based on the classical equilibrium MD simulations in accordance with the statistical mechanics theory, which uses the Einstein relation [38] or the Green-Kubo integral formula [39], [40]. The Einstein relation connects the diffusion coefficient to the slope of the mean square displacement of the diffusing particle trajectory, while the Green-Kubo integral formula calculates the same based on the integral of the velocity autocorrelation function. For numerical simulations, the Einstein method often appears more preferable in comparison with the Green-Kubo method since the particle coordinates can be calculated more accurately in comparison with the particle velocities which involve an extra differentiation [41]. The Einstein relation method is selected for computing the diffusion coefficients in the simulations based on the hybrid multi-scale method in the present work.

The current hybrid method is based on the two-phase flow analogy method for smoothly coupling the continuum mechanics description with MD via a specific buffer zone, which was first introduced in [42] and subsequently tested for a number of idealised molecular systems in [43], [44]. Within this framework, thermal fluctuations and other unsteady fluid mechanics effects are included by assuming that the continuum mechanics part of the model is governed by the Landau and Lifshitz Fluctuating Hydrodynamics equations (FH) [45]. Similar to other state variable schemes, the method uses a hybrid zone for coupling the MD and continuum representations of the two fluids. An analogy with two-phase flow modelling is used in the formulation of the hybrid coupling scheme. By introducing an MD particle and a continuum representation of the same liquid, the analogy method is formulated as equations for local conservation of mass and momentum fluxes of a nominally two-phase flow in the entire computational domain. The concentration of the continuum part of the flow is a user-defined function that controls the local resolution of the multiscale model. The continuum phase is modelled with a Eulerian approach and the MD particle phase is modelled with a

Lagrangain description. The "phases" are assumed to be in equilibrium and finely mixed one with another so that the interface effects in the two-phase mixture are not relevant. To avoid the artificial phase separation and preserve the continuity of variances of macroscopic flow quantities across the different phases, forcing terms are introduced as sources and sinks in the conservation laws for mass and momentum without affecting the local conservation property. In a further work of the authors [46]–[48] a simplified, one-way coupled version of the original hybrid method was developed for 3D simulations in GROMACS [49], [50], a popular open-source MD software. The simplified implementation assumes no feedback from the microscopic MD part of the solution on the macroscopic hydrodynamic part and also uses discrete particles in the entire computational domain so that the computational saving may come purely from skipping the calculation of particle–particle interactions in the hydrodynamic part of the solution domain. Despite these drawbacks, the model showed promise for simulations of a PCV2 virus capsid in water [47], [48]. In particular, the hybrid model is shown to correctly reproduce a stable capsid in a small computational domain and capture the relevant macroscopic transport characteristics of water and ions through the virus capsid compared to the reference all-atom simulation. More recently, a triple-scale one-way coupled scheme that combines the two-phase hydrodynamic analogy approach with multi-resolution molecular dynamics simulations (AdResS) has been developed [51]. By accounting for a smoother transition between the multi-atom water molecules to hydrodynamic particles in the flow, the triple-scale scheme is shown to lead to a reduced sensitivity to the model parameters while achieving an improved accuracy in test problems in comparison with the baseline MD-FH algorithm. A fully coupled two-phase analogy model for argon has also been implemented with taking into account the feedback of MD particles on the flow in [52]. The model demonstrated excellent accuracy for the Couette problem of liquid argon flow.

In the present publication, the Couette flow implementation of the two-phase analogy method for water and peptide systems will be considered for the first time in the literature. For the current application, the one-way coupled acoustic analogy model [46], [47] will be extended to the shear corrected boundary conditions. After an appropriate calibration and validation of the suggested implemenation is completed, it will be applied to the simulation of a small peptide diffusion in water under the shear flow effect. The numerical results of molecular diffusion modelling in water will be compared with the reference data available in the literature [53]–[56].

The paper is organised as the following. Section 2.1 briefly introduces the theoretical background of the two-phase analogy method for coupling continuum and particle representations of liquids. A simplified version of the two-phase analogy method that leads to the one-way coupled MD-FH model is considered in section 2.2. An extension of the MD-FH model for the Couette flow is presented in section 2.3. In section 3, the results of the MD-FH model for the Couette flow are presented and discussed with reference to the all-atom MD simulations. The results include the comparison with the reference analytical solution for the meanflow velocity profile in subsection 3.1 and the study of water self-diffusion and a small protein diffusion in water in sections 3.2 and 3.3.

2. Theory

2.1 Two-phase analogy for coupling continuum and particle representations of the same liquid

The hybrid two-phase analogy model for multi-resolution simulations of liquids [42] is summarised as follows. Large-scale continuum and fine-scale particle representations of the same chemical substance are considered as 'phases' of the same nominally two-phase fluid,

which are immersed into each other without any phase separation. The concentration of the continuum phase and the particle phase are $0 \leq s \leq 1$ and $0 \leq 1\text{-}s \leq 1$, respectively, where s is a user-defined function of space and time that describes which part of the volume is represented by discrete particles and which by continuum. For example, in [47] the s-function was selected as a spherical distribution in space whose centre is locked with the centre of mass of a peptide molecule of interest that moves in water in accordance with the diffusion process.

The process of phase mixing, which corresponds to changing of the model resolution, is specified by the sources on the right-hand-side of the mass and momentum equations of the phases. Under assumption that there are no macroscopic temperature gradients, the macroscopic temperature equation is irrelevant. This leads to a closed system, which contains the conservation equation of mass of the continuum phase,

$$\delta_t(sm) + \sum_{\gamma=1,6} \left(s\rho\bar{\mathbf{u}} \right) d\mathbf{n}^\gamma \delta t = \delta_t J^{(\rho)} \tag{1}$$

the equation of mass of the particle phase,

$$\delta_t \left((1-s) \sum_{p=1,N(t)} m_p \right) + \sum_{\gamma=1,6} \left((1-s) \sum_{p=1,N_\gamma(t)} \rho_p \mathbf{u}_p \right) d\mathbf{n}^\gamma \delta t = -\delta_t J^{(\rho)}, \tag{2}$$

the equation of momentum of the continuum phase,

$$\delta_t(smu_i) + \sum_{\gamma=1,6} \left(s\rho u_i \bar{\mathbf{u}} \right) d\mathbf{n}^\gamma \delta t = s \sum_{j=1,3} \sum_{\gamma=1,6} \left(\Pi_{ij} + \tilde{\Pi}_{ij} \right) dn_j^\gamma \delta t + \delta_t J_i^{(\mathbf{u})}, \tag{3}$$

and that of momentum of the particle phase

$$\delta_t \left((1-s) \sum_{p=1,N(t)} m_p u_{ip} \right) + \sum_{\lambda=1,6} \left((1-s) \sum_{p=1,N_\gamma(t)} \rho_p u_{ip} \mathbf{u}_p \right) d\mathbf{n}^\gamma \delta t = (1-s) \sum_{p=1,N(t)} F_{ip} \delta t - \delta_t J_i^{(\mathbf{u})}, \tag{4}$$

and which is formulated on a Eulerian grid of hexahedral control volumes, V.

Here the fields which correspond to the particles are with a sub-index p and those which stand for the cell-volume averaged and the cell-flux averaged quantities (e.g. obtained from an appropriate reconstruction inside each cell in accordance with a finite-volume method) are without the sub-index. $\gamma = 1,..,6$ are the faces of the control volume V, m and $\rho = m/V$ are the mass and density of the continuum phase of the elementary volume, m_p is the particle mass, $\mathbf{u}_p$ is the particle velocity, $\overline{\mathbf{u}}$ is the particle-continuum 'mixture' velocity,

$$\overline{u}_i = \left[s\rho u_i + (1-s) \sum_{p=1,N(t)} \rho_p u_{ip} \right] / \overline{\rho} \,, \, u_i \text{ is the velocity of the continuum phase, } \overline{\rho} \text{ is the}$$

mixture density, $\overline{\rho} = s\rho + (1-s) \sum_{p=1,N(t)} \rho_p$, $N(t)$ is the number of particles in the control volume V which typically is at least O(100) for statistical convergence of the FH solution. $N_\gamma(t)$ is the number of particles crossing the γth cell face with the area normal $d\mathbf{n}^\gamma$ at time t, $\rho_p = m_p / V$ is the effective density of particle p per volume V, δ_t describes the change of each quantity over time δt, e.g. counts the particle mass and momentum accumulated in cell V over time δt. F_{ip} is the total inter-particle interaction force exerted on particle p.

For the continuum phase momentum equation, the Landau-Lifshitz Fluctuating Hydrodynamics model is used, which is implemented by adding the random stress tensor, $\widetilde{\Pi}$ to the deterministic stress of the Navier-Stokes equations, Π in order to account for the effect of Brownian motion.

$\delta_t J^{(\rho)}$ and $\delta_t J_i^{(\mathbf{u})}$ are the mass and the momentum exchange terms between the two phases, which are a function of the user-defined phase concentration function s. These exchange terms control how fast the fine-scale particle phase ($s = 0$) is replaced by the large-scale

continuum phase ($s = 1$) in the computational domain to maintain a balance between the computational cost reduction and accuracy.

Important properties of the system of conservation laws (1)-(4) include conservation of mass $\bar{m} = \bar{\rho}V$ and momentum fluxes in accordance with Newton's second law that equates the change of the total momentum $\bar{m} \cdot \bar{\mathbf{u}}$ to the force applied,

$$\bar{F}_i = s \sum_{j=1,3} \sum_{\alpha=1,6} \left(\Pi_{ij} + \tilde{\Pi}_{ij} \right) dn_j^\alpha \delta t + (1-s) \sum_{p=1,N(t)} F_{ip}.$$

The two-phase analogy model is closed by defining the particle-particle interaction model (e.g. in accordance with classical Molecular Dynamics) and introducing the appropriate continuum-discrete source fields in the kinematic and dynamic equation for each particle so that, collectively, the particle phase satisfies the governing conservation laws (1)-(4).

2.2 A single-resolution particle liquid in the fluctuating hydrodynamics bath

Following the assumptions considered in [46], the effect of discrete particles on the macroscopic hydrodynamics is ignored, and the dependent variables of the hybrid two-phase mixture, $\bar{\rho}$ and $\bar{u}_i$ are replaced by the solution of the Landau-Lifshitz Fluctuating Hydrodynamics (LL-FH) model that represents the statistical properties of liquids at mesoscale:

$$\begin{aligned}
&\frac{\partial \bar{\rho}}{\partial t} + div\left(\bar{\rho} \cdot \bar{\mathbf{u}} \right) = 0, \\
&\frac{\partial \left(\bar{\rho} \cdot \bar{u}_i \right)}{\partial t} + div\left(\bar{\rho} \cdot \bar{u}_i \cdot \bar{\mathbf{u}} \right) = \sum_{j=1,3} \nabla_j \left(\Pi_{ij} + \tilde{\Pi}_{ij} \right), \ i = 1, 2, 3
\end{aligned} \tag{5}$$

Here $\bar{p} = \bar{p}(\bar{\rho})$ in accordance with the equation of state, the stress tensor $\mathbf{\Pi}$ and its fluctuating component $\widetilde{\mathbf{\Pi}}$ are defined so that

$$\Pi_{i,j} = -\left(\bar{p} - \zeta \, div\, \bar{\mathbf{u}}\right)\delta_{i,j} + \eta\left(\partial_i \bar{u}_j + \partial_i \bar{u}_j - 2D^{-1} div\, \bar{\mathbf{u}} \delta_{i,j}\right),$$

$$\tilde{\Pi}_{i,j} = \zeta \, div\, \tilde{\mathbf{u}} \delta_{i,j} + \eta\left(\partial_i \tilde{u}_j + \partial_i \tilde{u}_j - 2D^{-1} div\, \tilde{\mathbf{u}} \delta_{i,j}\right), \quad i,j = 1,2,3 \tag{6}$$

where η and ζ are shear and bulk viscosity coefficients, D is the spatial dimension. $\tilde{\mathbf{\Pi}}$ is

modelled as a random Gaussian matrix with zero mean and covariance:

$$\left\langle \tilde{\Pi}_{i,j}(\mathbf{r}_1,t_1)\tilde{\Pi}_{k,l}(\mathbf{r}_2,t_2)\right\rangle = 2k_B T \left[\eta\left(\delta_{i,k}\delta_{j,l} + \delta_{i,l}\delta_{j,k}\right) + \left(\zeta - 2D^{-1}\eta\right)\delta_{i,j}\delta_{k,l}\right]\delta(t_1 - t_2)\delta(\mathbf{r}_1 - \mathbf{r}_2). \tag{7}$$

Following [45], the stochastic stress tensor is represented explicitly so that

$$\tilde{\Pi}_{i,j} \cong \sqrt{\frac{2k_B T}{\delta t \delta V}}\left(\sqrt{2}\sqrt{\eta} \cdot G_{i,j}^S + \sqrt{D}\sqrt{\zeta} \cdot tr[\mathbf{G}] \cdot E_{i,j} / D\right), \quad i,j = 1,2,3 \tag{8}$$

where $\mathbf{G}$ is a random Gaussian matrix with zero mean and covariance $\left\langle G_{i,j}G_{k,l}\right\rangle = \delta_{i,j}\delta_{k,l}$,

$G_{i,j}^S = \dfrac{G_{i,j} + G_{i,j}^T}{2} - tr[\mathbf{G}] \cdot E_{i,j} / D$, is a random symmetric matrix with zero trace, $\mathbf{E}$ is the

identity matrix, and $tr[\mathbf{G}]$ is the trace of the matrix $\mathbf{G}$.

The above leads to the one-way coupled MD-FH model when the hydrodynamic equations

(5)-(8) are solved with a central finite-volume method [57]. The time step of the FH solution

is 10 times larger in comparison with the MD step. For given O(100) particles per control

volume the cost of solving the LL-FH equations is negligible in comparison with the MD

simulation. The FH solution provides an effective hydrodynamic "bath" for particle

"binding" with continuum hydrodynamics of Non-Equilibrium Molecular Dynamics

(NEMD)-type in accordance with the equations for particle coordinates and velocities:

$$\frac{d\mathbf{x}_p}{dt} = \mathbf{u}_p + \mathbf{Q}_1,$$

$$\frac{d\mathbf{u}_p}{dt} = \mathbf{Q},$$

$$\mathbf{Q}_1 = s(\bar{\mathbf{u}} - \mathbf{u}_p) + s(1-s) \cdot \alpha \cdot \frac{\sum_{\gamma=1,6}\left(\bar{\rho} - \sum_{q=1,N_\gamma(t)} \rho_q\right) d\mathbf{n}^\gamma}{\sum_{q=1,N(t)} m_q} \tag{9}$$

$$Q_i = (1-s)F_{ip}/m_p + \sum_{k=1,3}\sum_{\gamma=1,6}\left(s(1-s)\cdot\alpha\cdot\sum_{q=1,N_\gamma(t)}\rho_q u_{iq}\cdot\left(\frac{\sum_{\lambda=1,6}\left(\bar{\rho}-\sum_{q=1,N_\lambda(t)}\rho_q\right)dn_k^\lambda}{\sum_{q=1,N(t)}m_q}\right)\right)dn_k^\gamma/\sum_{q=1,N(t)}m_q$$

$$+\sum_{k=1,3}\sum_{\gamma=1,6}\left(s(1-s)\cdot\beta\cdot\frac{1}{V}\left(\sum_{\lambda=1,6}\left(\bar{\rho}\cdot\bar{u}_i-\sum_{q=1,N_\lambda(t)}\rho_q u_{iq}\right)dn_k^\lambda\right)\right)dn_k^\gamma/\sum_{q=1,N(t)}m_q,\quad i=1,2,3.$$

Here, the macroscopic fields correspond to control volume-averaged values and conservative fluxes are defined through the six sides of each control volume in accordance with the area normal $d\mathbf{n}^\gamma$, $\gamma=1,..,6$. All fields are interpolated to the current particle location. For simplicity, all functions inside the cell are reconstructed via a linear interpolation and the values of the fluxes are computed by interpolation in accordance with a central finite-volume scheme. $\alpha, \beta > 0$ are adjustable parameters that correspond to how fast the particle phase is forced to 'diffuse' to the Fluctuating Hydrodynamics solution in the hybrid region 0<s<1.

If the no-flow case considered by [46], [47], and [48] the continuum velocity and the density field, $\bar{\mathbf{u}}$ and $\bar{\rho}$, correspond to the zero-mean velocity fluctuations and the fluctuating density field in accordance with the equilibrium solution at given temperature, which are obtained from the numerical solution of the governing hydrodynamic equations (5-8).

Further following [46], [47], and [48], the inter-particle interaction forces, F_{ip} are defined in accordance with the classical Molecular Dynamics and Eq. (9) is integrated with the standard velocity Verlet algorithm [58].

The free parameters of the one-way coupling scheme, α and β are adjusted within the range of 10-100 nm^{2}ps^{-1}. Specific values depend on the application to achieve a sufficiently smooth but strong "phase binding" in each case.

2.3 Adaptation of the MD-FH model to the Couette flow problem

Let us consider a rectangular solution domain, where the flow is applied in the x_1-direction and the velocity gradient is applied in the x_2-direction, where $0 \leq x_2 \leq L$ and L is the size of the flow domain in the transverse flow direction. x_3 is a homogeneous direction. Standard periodic boundary conditions are assumed in the x_1- and x_3- directions. The applied velocity strain is such that the achieved flow velocity at the bottom and the top walls of the domain are $-V_{\max}$ and $V_{\max}$, respectively, which corresponds to a zero velocity of the system centre mass. For all numerical examples considered in the current publication, $V_{\max}$ is 0.05 nm/ps and L is 7 nm.

For the steady shear flow conditions, the density is not affected by the shear but the hydrodynamic velocity solution needs to include the velocity strain component $\delta u_1(x_2)$ in comparison with the no-flow case. In comparison with Eq(9), this leads to a modification of the corresponding particle coordination equation in the flow direction, x_1

$$\frac{dx_{1p}}{dt} = u_{1p} + Q_{11},$$

$$Q_{11} = s\left[\left(\bar{u}_1 + \delta u_1(x_2)\right) - u_{1p}\right] + s(1-s) \cdot \alpha \cdot \frac{\sum\limits_{\gamma=1,6}\left(\bar{\rho} - \sum\limits_{q=1,N_\gamma(t)}\rho_q\right)d\mathbf{n}^\gamma}{\sum\limits_{q=1,N(t)}m_q} \qquad (10)$$

where

$$\delta u_1(x_2) = \gamma x_2 - V_{max} \tag{11}$$

and γ is the velocity strain, which is equal to $\dfrac{2V_{max}}{L}$.

Following previous implementations of the analogy method [46], [47], and [48], a spherical-shape user-defined function $s = s(\mathbf{x}, t)$ is specified so that it is zero in the centre of the computational domain and grows to the domain periphery where the particles are driven by the "external" hydrodynamic field:

$$s(r) = \begin{cases} S_{min}, & r \le R_{MD}; \\ \dfrac{r - R_{MD}}{R_{FH} - R_{MD}} \left(S_{max} - S_{min} \right) + S_{min}, & R_{MD} < r < R_{FH}; \\ S_{max}, & r \ge R_{FH}. \end{cases} \tag{12}$$

where R_{MD} and R_{FH} are the radii of the discrete particle and the hydrodynamic zone which are user-defined parameters, r is the distance to the geometrical centre of discrete particle zone. The limiting values of the s-function used in the current model are $S_{min} = 0, S_{max} = 0.98$ (fig. 1a). Depending on the application, the geometrical centre either corresponds to the geometrical centre of the simulation domain or is locked to the centre of mass of a molecular system of interest (e.g. a moving peptide molecule considered in section 3.2).

Periodic boundary conditions for particles are specified in all three directions of the computational domain. While the standard periodic conditions are applicable in the streamwise and the spanwise directions, x_1 and x_3, a shear-corrected periodic boundary condition is required in the x_2-direction.

First of all, it can be noted that particles on the top boundary and on the bottom boundaries of the computational domain correspond to different flow velocities in the x_1-direction. The

16

velocity difference leads to an offset distance in the x_1-coordinate that accumulates when recycling a particle from one boundary to another in accordance with the periodic condition in the x_2-direction. The offset distance d depends on the gradient of the flow, the size of the box, and the integration time step of MD particles:

$$d = \gamma L \cdot \Delta t = 2V_{max} \cdot \Delta t \qquad (13)$$

The integration time step of the current model, which has been adjusted for stability, is 0.001 ps and the maximum velocity, V_{max} is 0.05 nm/ps, which leads to the offset distance d being very small in comparison with the intermolecular distance. Hence d is neglected in the current simulations.

The adjustment of the periodic boundary conditions in the transverse direction that is required, however, is to strictly enforce the effective non-slip condition at the top and the bottom flow wall for the particles. The particle velocity at the boundaries need to be rescaled for making sure that the mean particle velocities at the top and bottom boundaries of the computational domain are equal to the prescribed flow stream velocities. The rescaling correction is needed in addition to the current diffusion-based "binding" of the MD particles with the Fluctuating Hydrodynamics region of the hybrid model. The "diffusion" treatment is required to be sufficiently soft for a smooth particle transition from one representation to another and cannot strictly enforce the non-slip condition required for the Couette flow problem without the additional boundary correction.

The enforcing of the non-slip boundary condition for particles is implemented as follows. The entire computational domain is divided into 16 layers in the transverse direction. The instantaneous mass-weighted average particle velocity in the flow direction of each layer

$\bar{u}_{layer,j}$ is calculated by summing up the corresponding contributions of all particles and then dividing the sum by the total mass of the layer:

$$\bar{u}_{layer,j} = \frac{\sum_{p=0}^{N_j} m_p u_{1p}}{\sum_{p=0}^{N_j} m_p} \tag{14}$$

Here j stands for the layer number, $0 \le j \le 16$, N_j is the number of particles per layer, m_p and u_{1p} are the mass and the x_1-velocity component of particle p of the layer.

In order to enforce the appropriate shear-corrected boundary condition, the particle velocity fluctuation, u'_{1p} is computed by subtracting the average velocity of all particles in the top and in the bottom layer from the MD particle velocity:

$$u'_{1p} = u_{1p} - \bar{u}_{layer,j} \tag{15}$$

The above quantity is computed for all particles within a distance of 2 nm from the top or bottom boundary, which is within the effect of the periodic boundary condition. The corrected velocity of the boundary layer particles is defined as a sum of the computed velocity fluctuation and the meanflow velocity in accordance with the analytical solution

$$u_{1p} \equiv u'_{1p} + \delta u_1(x_2)$$

so that near the boundaries the shear-corrected coordinate equation (10) is replaced by:

$$\frac{dx_1}{dt} = (1-s)u'_{1p} + s\bar{u}_1 + \delta u_1(x_2) + s(1-s) \cdot \alpha \cdot \frac{\sum_{\gamma=1,6}\left(\bar{\rho} - \sum_{q=1,N_\gamma(t)}\rho_q\right)d\mathbf{n}^\gamma}{\sum_{q=1,N(t)} m_q}, \tag{16}$$

3 Validation

3.1 Initial calibration of the MD-FH model

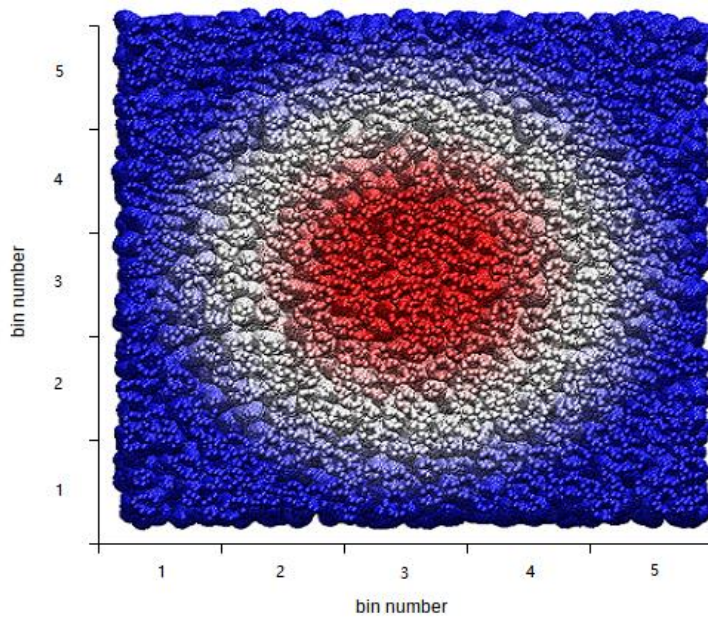<u>A. Water at equilibrium conditions</u>

As discussed in [51], accuracy of the one-way coupled MD-FH method for multi-resolution simulations of water is sensitive to calibration parameters such as the spatial width of the hybrid zone where $S_{min} < s < S_{max}$ as well as the size of the pure MD zone, which are determined by R_{MD} and R_{FH} parameters of the s-function (12).

For the validation purposes, the test case of simulating water at equilibrium conditions corresponding to room temperature, T=298K is considered first. The spherical-shape distribution of the s-function is specified in the centre of the cubic computational domain $(7.19 \text{ nm})^3$ with periodic boundary conditions in all 3 coordinate directions. Fig.1a shows initial distribution of MD particles where the pure MD zone (red) gradually merges with the hybrid atomistic-continuum zone (white) and then with the hydrodynamics region (blue). In the MD simulation, Extended Simple Point Charge (SPC/E) water model is used. The standard Nose-Hover thermostat is applied and the reference temperature is 298.15 K. The MD integration time step is 2 fs, and the total simulation time is 1 ns. The reaction field electrostatics is applied where the cut-off length is 1.0 nm, the dielectric constant is 78, and the van der Waals cut-off length is 1.0 nm. For solving the hydrodynamic equations, the entire solution domain is decomposed into 5^3 control volumes or MD "bins". The α and β parameters of the hybrid coupling scheme are set to 100 $\text{nm}^2\text{ps}^{-1}$.

An important property of a scale-resolved model is to correctly capture the radial distribution function (RDF) and velocity autocorrelation functions (VACFs). In application to the suggested MD-FH model, this means a correct preservation of RDF and VACF functions in the inner all-atom MD region (s=0) to investigate if these functions are not affected by proximity of the hybrid region of the model. Fig.1b,c shows results of analysis for a probe

point location in the inner MD zone where the RDF and VACF distributions are extracted for oxygen. The parameters of the hybrid zone of the MD-FH model are $R_{MD} = 0.3L/2$ and $R_{FH} = 0.8L/2$, where L is the size of the computational domain, L =7.19 nm.

The obtained distributions of RDF and VACF are in a good agreement with the reference all-atom MD simulations. Following [51], the standard deviations of density and velocity of the pure MD zone of the hybrid method solution have also been verified to be in a good agreement with the reference all-atom MD solution. The results of this test have provided typical values of the hybrid model parameters when the accuracy of the method for multi-resolution water simulations could be sufficient.
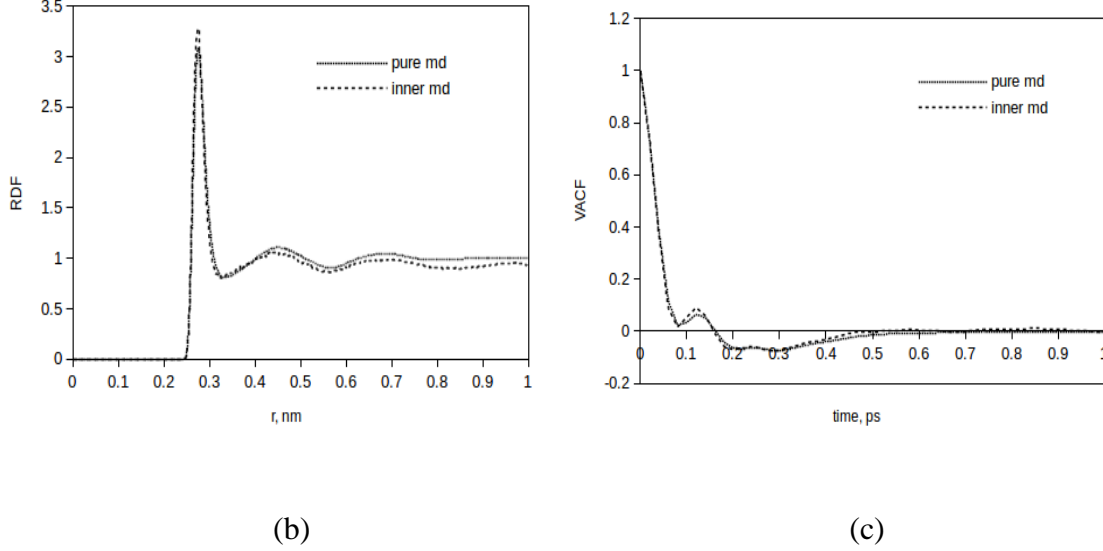

(a)

(b)	(c)

Figure 1. Initial testing of the hybrid MD-FH method for water in equilibrium conditions: domain decomposition of the computational domain that includes the pure MD region (red) where $s = 0$, the hybrid zone (white) where s gradually changes from 0 to s_{max}, and the hydrodynamics-dominated zone where $s = s_{max}$ (blue) (a) and comparisons of the obtained RDF (b) and VACF (c) distributions for oxygen atoms in the inner pure MD region with the "true" distributions obtained from the reference all-atom MD simulation.

B. Steady Couette flow problem

The same hybrid water model is now considered under the steady Couette flow conditions as discussed in Section 2.3. The initial condition corresponds to zero flow as for the equilibrium water system shown in fig.1a. The flow is started impulsively by specifying the constant velocity in the entire fluid volume in accordance with the modified coordinate equations (10), (11), and (16). A typical instantaneous distribution of water molecules affected by the velocity strain is shown in fig. 2a. The original spherical distribution of the MD particles (red) and the hybrid (white) zone is reshaped consistently with the drag applied through the non-

slip boundary conditions on the top and the bottom boundaries. The colours correspond to distribution of MD particles in the solution domain at the initial time moment (fig.1a). Hence, the mixture of red and white "solute" in the initial central zone shows that the MD particles freely migrate from the pure MD zone to the continuum mechanics periphery and back in accordance with the governing equations.

It should be pointed out that despite the atoms in the pure MD zone rapidly mix out with the surrounding MD particles in the continuum zone under the shear flow effect, the number of "fully-atomistic" particles in the pure MD zone remains approximately the same. This is because the total number of MD particles in the simulation does not change because of the periodic boundary conditions and the "washed away" MD atoms being quickly replaced by the particles coming to the fully atomistic region from the hydrodynamic region. The particle exchange mechanism is driven by the MD-FH forcing at the periphery of the pure MD zone that has been appropriately calibrated to prevent the artificial "phase separation".

It should be pointed out that the forcing terms of the current MD-FH model is identically zero in the pure MD region, hence, the atoms in MD region are accelerated by the flow through their interaction with the particle-hydrodynamic region at the periphery. That is, there is no artificial forcing applied to the atoms in the pure MD domain, which is simulated in a full accordance with the inter-atomic potentials of the standard equilibrium molecular dynamics. This can be compared with some of the Non-Equilibrium MD methods which apply an artificial force on all atoms directly to simulate the flow effect [59]–[61].

For smooth transition from one description to another, the α and β parameters of the hybrid algorithm are adjusted to the lower end of their range so that they are both equal to 10 nm^{2}ps$^-$^{1}. The MD integration time step is reduced to 1 fs for stability. It can be noted that both

adjustments are required due to simplicity of the current hybrid model in comparison with more sophisticated models such as those considered by [51] and [52].

Accuracy of the MD-FH model for the steady Couette problem is assessed by comparing the meanflow velocity profile across the transverse direction of the computational domain with the analytical solution. As described in Section 2.3, the whole domain is split into 16 layers in the transverse direction and the mean particle velocity in the flow direction is calculated at each integration time step in each layer. After appropriate time averaging, the resulting meanflow velocity profile is compared with the analytical solution.

In order to estimate how effectively MD atoms get entrained in the shear flow, sensitivity of the hybrid model solution to the size of the hybrid MD/hydrodynamic zone is investigated. Two different combinations of R_{MD} and R_{FH} parameters of the hybrid model are examined. The two cases correspond to the same radius of the pure MD region R_{MD} equal to $0.3L/2$ and different radius of the external hydrodynamic zone, R_{FH} which varies from $0.6L/2$ to $0.8L/2$. Fig. 2b shows that the meanflow velocity profiles corresponding to the two configurations of the hybrid model are in a good agreement with the analytical solution. This confirms a moderate sensitivity of the solution to the width of the hybrid zone around the considered range of parameters.
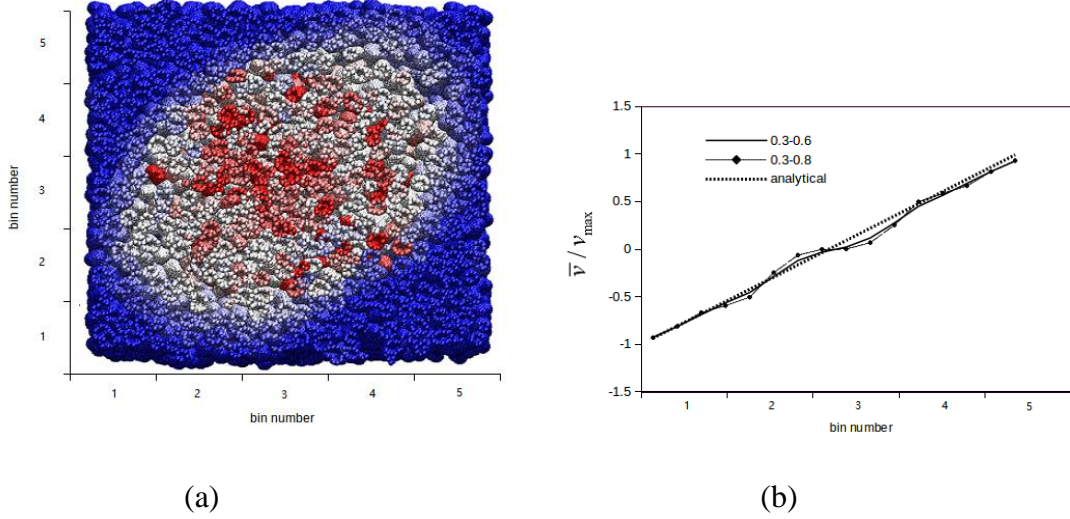
(a)   (b)

Figure 2. Hybrid MD-FH method for water simulation under velocity strain: a typical distribution of water molecules in the hybrid MD-FH domain after 10 ps since the start of the simulation (a) and comparison of the meanflow velocity profile with the analytical solution for different configurations of the hybrid model, where the first and the second number in the hybrid solution legend corresponds to the ratios of the MD zone and the hydrodynamic zone sizes to the full domain size, $2R_{MD} / L$ and $2R_{FH} / L$, respectively.

3.2 Effect of the flow velocity strain on molecular diffusion
A. Analytical modelling

Following [32] and [33] with assuming that diffusion process is isotropic, e.g. in the absence of the strain field [62], analytical expressions for mean square displacements of the diffusing particles can be obtained:

$$
\begin{aligned}
\left\langle x_1^{2}(t)\right\rangle &= 2Dt + \frac{2}{3}D\gamma^{2}t^{3}, \\
\left\langle x_2^{2}(t)\right\rangle &= 2Dt, \\
\left\langle x_3^{2}(t)\right\rangle &= 2Dt, \\
\left\langle x_1(t)x_2(t)\right\rangle &= D\gamma t^{2}
\end{aligned}
\tag{17}
$$

where $\langle\;\rangle$ stands for particle ensemble averages and D is diffusion coefficient.

In assumption that the diffusion tensor is diagonal but not necesserily isotropic the above expressions are modified by [56]:

$$\boldsymbol{D} = \begin{bmatrix} D_{x_1 x_1} & 0 & 0 \\ 0 & D_{x_2 x_2} & 0 \\ 0 & 0 & D_{x_3 x_3} \end{bmatrix} \tag{18}$$

and

$$
\begin{aligned}
\left\langle x_1^2(t) \right\rangle &= 2D_{x_1 x_1} t + \frac{2}{3} D_{x_2 x_2} \gamma^2 t^3, \\
\left\langle x_2^2(t) \right\rangle &= 2D_{x_2 x_2} t, \\
\left\langle x_3^2(t) \right\rangle &= 2D_{x_3 x_3} t, \\
\left\langle x_1(t) x_2(t) \right\rangle &= D_{x_2 x_2} \gamma t^2
\end{aligned}
\tag{19}
$$

For the steady Couette flow problem of interest in the current publication, the following expression for the mean square particle displacement in the flow direction as a function of the mean square displacement without the convection effect, $\left\langle \Delta q_1^2(t) \right\rangle$ can be further obtained [56]:

$$
\begin{aligned}
\left\langle \Delta x_1^2(t) \right\rangle &= \left\langle \Delta q_1^2(t) \right\rangle + \lambda \cdot t^2 + \gamma \left\langle \Delta q_1(t) \Delta x_2(t) \right\rangle t, \\
\lambda &= \gamma^2 \left\langle x_2^2(0) \right\rangle + \frac{\gamma^2}{3} \left\langle \Delta x_2^2(t) \right\rangle
\end{aligned}
\tag{20}
$$

For Newtonian liquids, such as water at normal conditions, the correlation $\left\langle \Delta q_1(t) \Delta x_2(t) \right\rangle$ is neglected and the mean square displacement in the homogeneous flow direction, $\left\langle x_3^2(t) \right\rangle$ is not affected by the flow. This leads to an explicit relation between the mean square particle displacement in the flow direction, $\left\langle x_1^2(t) \right\rangle$ and the homogeneous flow direction, $\left\langle x_1^2(t) \right\rangle$ as follows:

$$\left\langle \Delta x_1^{\,2}(t) \right\rangle = \left\langle \Delta x_3^{\,2}(t) \right\rangle + \lambda \cdot t^2 \qquad (21)$$

The same relation can be obtained from the simple analytical model based on the idea of scale decomposition as described below:

Let us assume that the velocity of a diffusing particle consists of two components, the small-scale random diffusion velocity $\mathbf{u}_d$ and the large-scale convection flow velocity $\mathbf{u}_c$ induced due to the macroscopic flow effect:

$$\mathbf{u}_p = \mathbf{u}_d + \mathbf{u}_c \qquad (22)$$

where the convection velocity is $\mathbf{u}_c = (u_{1c}, 0, 0)$ and equal to the mean particle velocity, $\left\langle \mathbf{u}_p \right\rangle$.

Here $\left\langle \; \right\rangle$ means the paricle ensemble averaging.

By integrating equation (22) in time, an equation for particle coordinate in the flow direction follows,

$$x_{1p}(\tau + t) = x_{1p}(\tau) + \int_{\tau}^{\tau+t} u_{1d} \cdot dt' + \int_{\tau}^{\tau+t} u_{1c} \cdot dt' \qquad (23)$$

By definition, the mean-square particle displacement in the flow direction is

$$\left\langle \Delta x_1^2(t) \right\rangle = \left\langle (x_{1p}(\tau + t) - x_{1p}(t))^2 \right\rangle ,$$

which using (23) is identical to

$$\left\langle \Delta x_1^2(t) \right\rangle = \left\langle \left(\int_{\tau}^{\tau+t} u_{1d} \cdot dt' + \int_{\tau}^{\tau+t} u_{1c} \cdot dt' \right)^2 \right\rangle . \qquad (24)$$

By re-arranging the right-hand-side of equation (24) and recalling that the radom diffusion velocity corresponds to zero mean, e.g. $\left\langle u_{1d} \right\rangle = 0$, the following expression for the mean square displacement in the flow direction is obtained

$$\left\langle \Delta x_1^2(t) \right\rangle = \left\langle \left(\int_\tau^{\tau+t} u_{1d} \cdot dt' \right)^2 \right\rangle + \left\langle \left(\int_\tau^{\tau+t} u_{1c} \cdot dt' \right)^2 \right\rangle, \tag{25}$$

where $\left\langle \left(\int_\tau^{\tau+t} u_{1d} \cdot dt' \right)^2 \right\rangle = \left\langle \Delta x_3^2(t) \right\rangle$ in accordance with the homogeneous flow assumption in

the x_3–direction and $\left\langle \left(\int_\tau^{\tau+t} u_{1c} \cdot dt' \right)^2 \right\rangle = \overline{u_{1c}^2} t^2$, where the overbar means the appropriate time

averaging. It can be noted that the above equation is identical to (21) with $\lambda \equiv \overline{u_{1c}^2}$.

To further progress with analytical modelling let us recall that instantaneous $u_{1c} = u_{1c}(x_{2p}(t))$

and assume that

$$\overline{u_{1c}^2} = \frac{\left\langle \left(\int_\tau^{\tau+t} u_{1c}(x_{2p}(t')) dt' \right)^2 \right\rangle}{t^2} \approx \frac{1}{L} \int_0^L \overline{\left(u_{1c}(x_{2p}(t)) \right)^2} dx_2 \tag{26}$$

where the overbar means time averaging.

Let us suppose there is an hydrodynamic focusing effect due to the shear flow on diffusing

particles so that their motion is restrained to a central slub of the Cuette flow domain away

from the moving "walls" in the x_2-direction. For example, let us assume that the duffusing

particles spend most of the time within a middle part of the solution domain

$-\varepsilon L/2 < x_3 - L/2 < \varepsilon L/2$, where $0 < \varepsilon < 1$.

By using (26) and recalling that $u_{1c}(x_{2p}(t)) = \gamma x_{2p}(t) - V_{max}$ and $V_{max} = \gamma L/2$, the square of

the effective convective velocity, $\lambda = \overline{u_{1c}^2}$ can be estimated from the following relation:

$$\lambda = \frac{2}{L} \int_0^{\frac{\varepsilon L}{2}} \left(\gamma x_2 - V_{max} \right)^2 dx_2 \tag{27}$$

which can be integrated analytically to obtain

$$\lambda = \frac{1}{3}V_{max}^{2}(1+(\varepsilon-1)^{3}) \qquad\qquad (28)$$

For the limiting cases, it can be noted that $\varepsilon=1$ corresponds to the diffusing particles being uniformly distributed across the flow domain and $\varepsilon=0$ corresponds to the situation when all the particles all clustered in the center of the flow where the effective convection velocity is zero.

B. Water self-diffusion with and without the shear flow

The effect of velocity strain on water self-diffusion properties is investigated using the hybrid MD-FH model of the steady Couette flow problem, which was considered in section 3.1B.

The translational self-diffusion coefficients D is obtained from the Einstein relation in accordance with the following expression for the Mean Square Displacement (MSD): $MSD(t) = \left\langle \Delta r(t)^{2} \right\rangle = A + 6Dt$. For validation purposes, the diffusion coefficient is first computed in the zero flow case as consdered by [46]. The MSD is calculated in the inner MD region of the stationary s-function distribution and the results are compared with the reference solution obtained from the all-atom MD simulation for water in Fig. 3 (b).

As noted by [46], the calculation of mean square deviation of water particles for self-diffusion is not straightforward. In comparison with the all-atom MD simulations, particles may freely leave and enter the hydrodnamic zone of the model, where the molecular diffusion in no longer resolved explicitly. For example, as soon as a molecule initiated in the pure MD domain center reaches periphery of the hybrid zone, the reminder of its trajectory is contaminated by hydrodynamics and cannot be used in the calculation of the molcular diffusion coefficient using the Einstein equation.

Only those particles which remain in the pure MD zone all time are considered in the particle ensemble averaging and a modifed routine for computing MSD in GROMACS has been used. The routine only considers a small part of the MD particles which are initially located in the central part of the pure MD domain within the radius of 0.3 nm (1-4 molecules). Furthermore, 10 short simulations (250 ps each) are run in order to limit the probability of the selected water molecules to leave the pure MD zone. The outcomes of the simulations are averaged to produce the resulting mean square deviation.

Fig.3a shows results of the mean square displacemment simulations for the three spatial directions, $\langle \Delta x_1^2(t) \rangle$, $\langle \Delta x_2^2(t) \rangle$, and $\langle \Delta x_3^2(t) \rangle$ as well as the total MSD(t) equal to the sum of the three. It can be noted that the three MSD corressponding to different directions of the isotropic space are very similar as expected. This suggests the statistical convergence obtained is reasonable and there are no notable artefacts which would skew the symmetry. To analyse how much the MSD trajectories of the hybrid solution are contaminated by the interaction with hydrodynamics, fig.3b compares the total MSD results of typical 5 short simulations with the avearged MSD trajectory which was produced from the reference all-atom MD simulation. The fluctuations at the end parts of the trajectories in fig.3b come from the hydrodynamic region effects. From comparison of fig.3a and b, it can be seen that at 100ps most MSD trajectories of the hybrid solution overpredict the mean square displacement of the all-atom MD solution by about 30%, which approximately is the same error in diffusion coefficient as reported by [46].

It should be noted that the water self-diffusion coefficient obtained from the reference all-atom MD simulation, D=2.68·10^{-5}cm^2/s is in excellent agreement with the experimental measurements, D=(2.57 ±0.022)· 10^{-5}cm^2/s which were reported by [63] for the same temperature. This is despite the fact that in the current computations of the diffusion

coefficient there are no correction for finiteness of the periodic box domain used. On the other hand, as discussed in [64], the finite box size correction could be important for computing the diffusion coefficient in complex fluids such as a polymer chain consisting of 30 monomers in a solvent. This suggests that, for diffusion computations in "simple fluids" like water, the finite-side box effect is not very important. Furthermore, it can be reasonably assumed that the diffusion computation in water that contains a small peptide molecule is neither strongly affected by the finite size of the computational box domain.

Having validated results of the present hyrbid method for the zero-flow case, the mean square deviations are computed for the steady Couette flow. Fig.3c shows the corresponding MSD solutions obtained for the flow direction, x_1, the transverse flow direction, x_2, and in the homogenuous flow direction, x_3. It can be seen that the MSD trajectory in the direction transverse to the flow has some higher slope than that in the spanwise x_3 direction, which is consistent with the literature [56]. Notably, the mean square deviation in the flow direction grows fastest due to the flow convection as expected. Fig.3d compares the MSD trajectory in the flow direction with a fitted curve in accordance with the theory, Eq.(21). The agreement with the fitted parabolic curve is reasonable over the first 60-70ps of the partcle trajectories where the diffusion results are not strongly contaminated by the hydrodynamic effects. This suggests that the simulated water flow has Newtonian properties as expected in the physical water experiment at normal conditions.
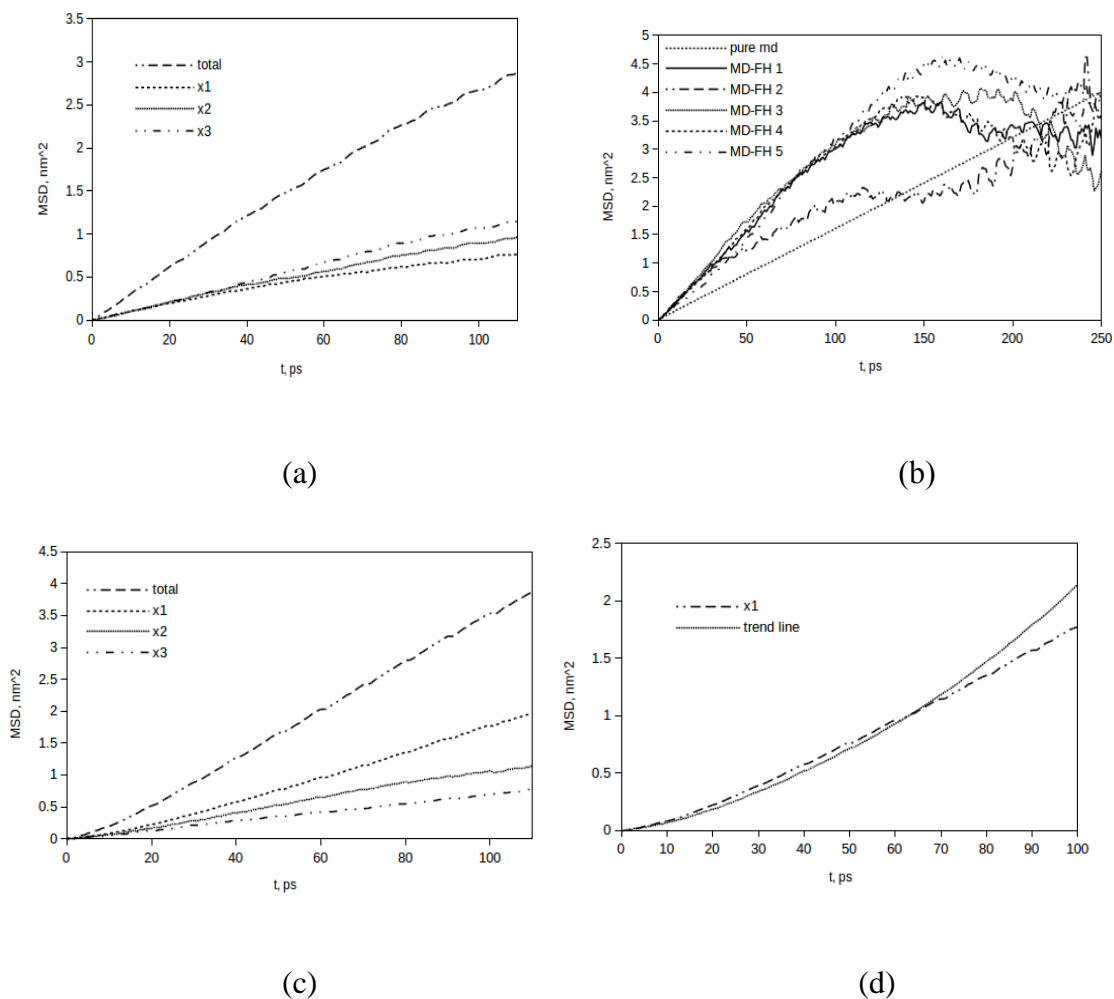
(a)

(b)

(c)

(d)

Figure 3. Effect of the flow on MSD trajectories: ensemble-averaged MSD trajectories from the hybrid method solution for water without flow along the x_1, x_2, and x_3 coordinate directions and the total MSD (a), typical samples of the total MSD trajectories in comparison with the reference all-atom total MSD solution with no flow applied (b), ensemble-averaged MSD trajectories along the x_1, x_2, and x_3 coordinate directions and the total for the shear flow applied (c), and the ensemble-averaged MSD trajectory along the x_1 direction and the fitted curve in accordance with the theoretical solution for Newtonian fluids (d).

C. Peptide diffusion in water with and without the shear flow

Following [46] a small peptide molecule in water is considered, which corresponds to the zwitterionic form of dialanine. Dialanine is the smallest protein consisting of only two aminoacid residues. It is popular for biomolecular research as it is simple and easy to analyse. In the present work, the zwitterion dialanine diffusion in water is simulated with and without the flow velocity strain effect.

Fig.4 shows the initial configuration of the MD-FH model where the solvated peptide molecule is introduced in the centre of the pure MD zone (comp. with fig.1a). Following [47], the centre of the pure MD zone in not fixed but locked to the centre of mass of the peptide so that the latter always remains surrounded by a water shell at all-atom resolution. After each time step when the peptide moves, the s-function (12) is recalculated accordingly. Such dynamic tracking allows one to use long trajectories of the peptide molecule when calculating its diffusion coefficient in comparison with using short data samples which were necessary for the stationary s-function case considered in Section 3.2B.

In comparison with the hybrid method configuration for pure water, the size of the pure MD region for the peptide case is increased to $R_{MD} = 0.5L/2$ while the size of the outer hydrodynamic shell is approximately the same, $R_{FH} = 0.8595L/2$. These empirical parameters were adjusted so that the hybrid method solution of the peptide diffusion in water at equilibrium conditions remains in a good agreement with the reference all-atom MD simulation. For improved statistical averaging, 10 independent simulations of the hybrid MD-FH model with a start from different realisations of initial conditions are performed, 1ns duration each. The ensemble averaged MSD results for the no flow case are shown in Fig. 5. In particular, fig. 5a shows that the MSD trajectories in three different coordinate directions are very close one to another, as expected from the no-flow case when the peptide diffusion should be isotropic. Again, the absence of notable asymmetries suggests that the parameters

of the hybrid method have been calibrated correctly and the ensemble averaged solutions are sufficiently converged. Fig. 5b illustrates the process of extracting the slope from the averaged total MSD trajectory from which the peptide diffusion coefficient is found in accordance with the Einstein relation. As predicted from the hybrid simulation, the diffusion coefficient value is $1.099 \times 10^{-5} cm^2 / s$. Given the uncertainty of the fit procedure, this predicted value is in a very good agreement with the reference all-atom MD simulation for the same system, which is $0.86 \times 10^{-5} cm^2 / s$.
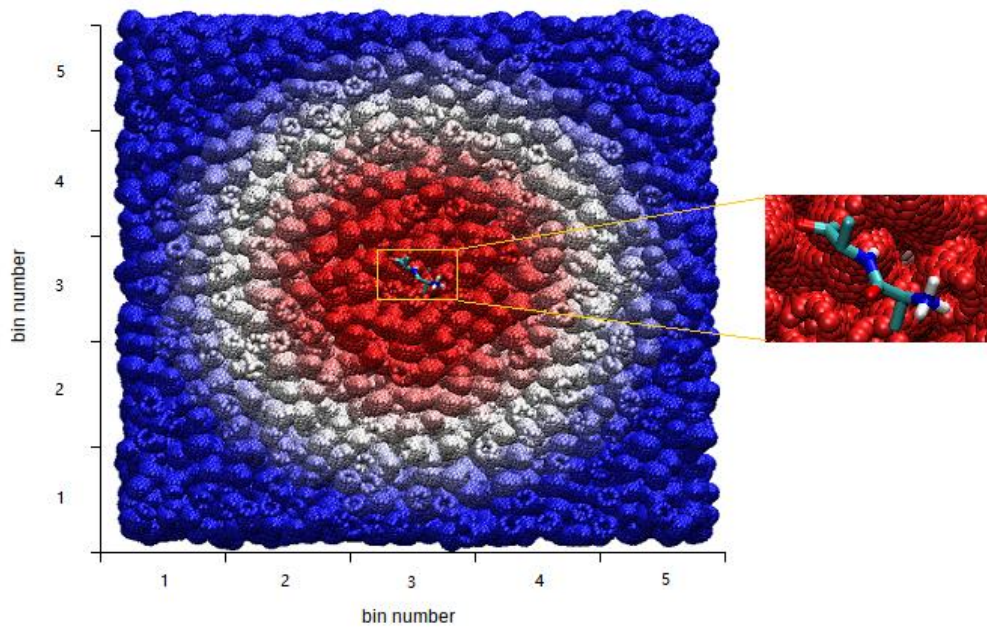
Figure 4. The hybrid MD-FH model of fig.1a with a small dialanine molecule immersed in water in the centre of the pure MD zone, which moves so that its centre is locked to the centre of mass of the molecule at all times.
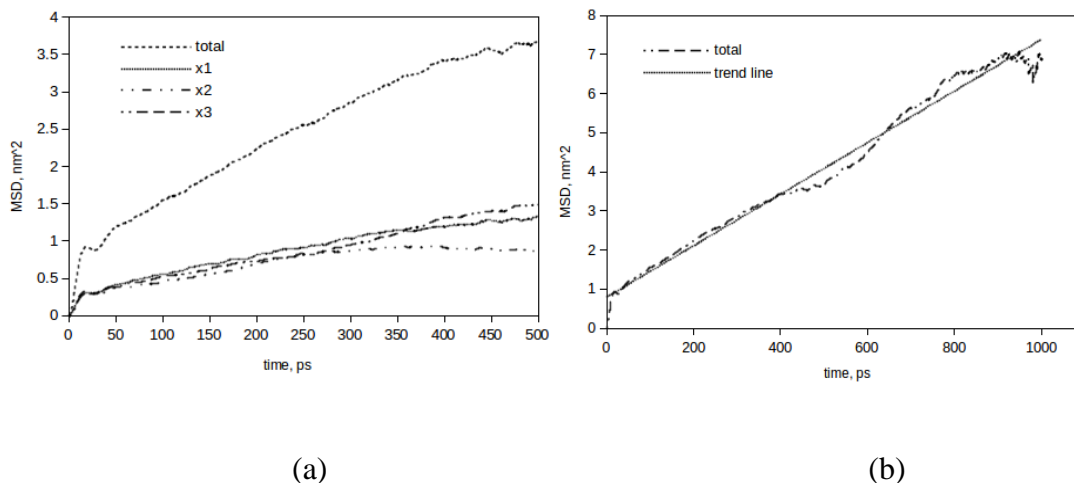
Figure 5. Hybrid method solutions for the peptide diffusion in water with no flow: ensemble averaged MSD trajectories along the x_1, x_2, and x_3 coordinate directions and the total (a) and the total MSD trajectory with a trend line extracted for calculation of the diffusion coefficient (b).

Finally, the same peptide in water is simulated under the steady Couette flow conditions by switching on the shear flow effects in accordance with equations (10), (11), and (16).

The same MSD calculation routine is applied to investigate the influence of the introduced strain field on the peptide diffusion and the results for different coordinate directions with respect to the flow are shown in fig. 6a. Again, it can be seen that the diffusion in the transverse x_2 direction is faster in comparison with the homogeneous flow direction, x_3. This is consistent with the literature [56] and is in-line with the results for water self-diffusion coefficients, which have been reported in section 3.2B.

The diffusion in both directions normal to the flow, x_2 and x_3 is much slower in comparison with the mean square displacement in the flow direction, x_1 that includes the flow convection effect and shows a non-linear growth with time. To quantify the latter time dependency,

fig.6b compares the MSD trajectory in the flow direction with a parabolic function fit based on the theoretical model (21) that is valid for Newtonian fluids. From a good agreement of the MSD trajectory with the analytical parabola curve it can be concluded that the compound fluid, which can be regarded as a much diluted protein water solution, exhibits similar Newtonian properties to the pure water. For accurate curve fitting, the fit parameter, λ is evaluated by re-arranging Eq(21) to a suitable form so that $\dfrac{\frac{1}{2}\log\left(\dfrac{\left\langle \Delta x_1^2(t)\right\rangle - \left\langle \Delta x_3^2(t)\right\rangle}{\lambda}\right)}{\log(t)} \approx 1$ as

shown in fig.6b. This results in the value of $\lambda = 0.1444 \cdot V_{max}^{\;2}$, which in accordance with Eq(28) gives $\varepsilon = 0.172 \square \; 1$. This value corresponds to the width of the flow domain, which is effectively occupied by the diffusing molecule. The value is notably less than one, which suggests that there is a marked hydrodynamic focusing effect on the peptide diffusion by the flow. The shear flow effect is such that the diffusing peptide molecule tends to be "sandwiched" within some 20% of the flow volume between the top and the bottom flow streams moving in opposite directions.

(a) (b)

35
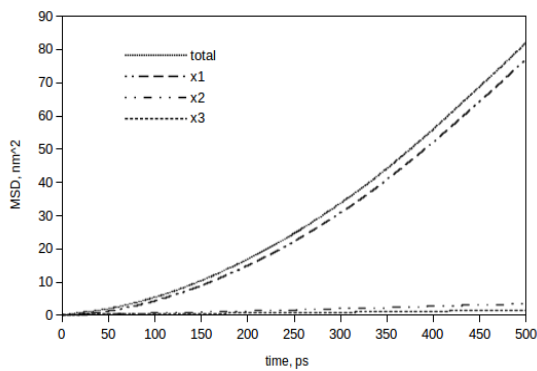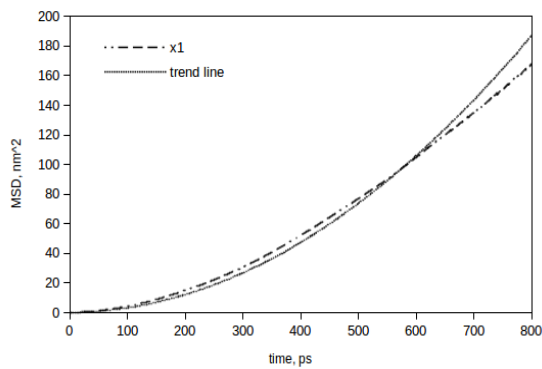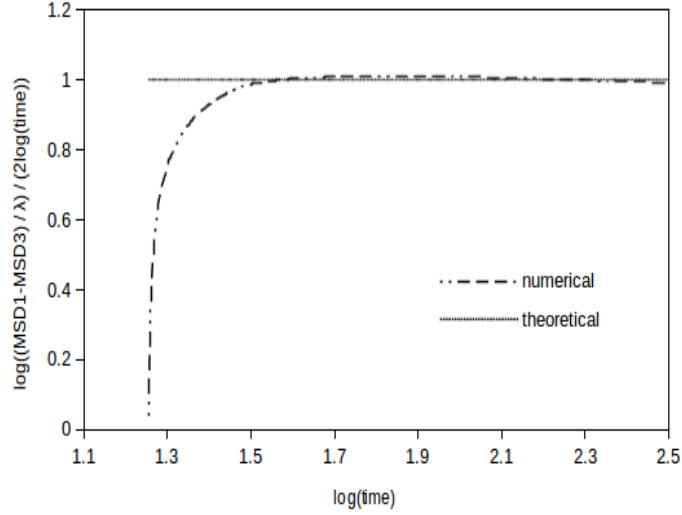
(c)

Figure 6. Hybrid method solutions for the peptide diffusion in water in the steady Couette flow: ensemble averaged MSD trajectories along the x_1, x_2, and x_3 coordinate directions and the total MSD (a) and the ensemble-averaged MSD trajectory along the x_1 direction and the fitted curve in accordance with the theoretical solution for Newtonian fluids (b),(c),

4 Conclusion

The Molecular Dynamics - Fluctuating Hydrodynamics (MD-FH) model has been extended for modelling of the velocity strain effect on molecular diffusion in water including self-diffusion and a small peptide molecule diffusion in water.

A one-way coupled model has been considered, where the MD particle equations are modified by the presence of hydrodynamic gradients in the coarse-grained part of the hybrid model. For the simulations, a small volume of the Couette flow is considered, which could be representative to a central section of a dual-stream laminar-flow micro-fluidic channel. An appropriate modification of the boundary conditions is implemented to strictly preserve the non-slip boundary condition at the moving "walls" in the transverse flow direction.

36

The hybrid model has been carefully calibrated to preserve the correct meanflow velocity profile. For the no-flow case, the radial distribution and the velocity autocorrelation functions as well as the water and peptide diffusion coefficients are in a good agreement with the reference all-atom MD simulations.

For diffusion simulations under the shear flow, predictions of the suggested hybrid model are in a qualitative agreement with the existing data in the literature. In particular, the molecular diffusion in the transverse flow direction is faster than that in the span-wise homogeneous flow direction and the diffusion in the flow direction includes the convection effect which is not correlated with the diffusion as expected for Newtonian flows.

A simple analytical model is proposed to elucidate the velocity strain effect on molecular diffusion for Newtonian fluids. The model is based on the idea of scale separation between the diffusion and convection processes and is in agreement with the existing theories of molecular diffusion in the literature. It has been used to quantify the effect of the peptide focusing by the hydrodynamic gradient in water as revealed in the present simulations: the diffusing peptide molecule is effectively "sandwiched" within some 20% of the flow volume between the top and the bottom flow streams moving in opposite directions.

Future work will be devoted to the implementation of more sophisticated versions of the two-phase flow analogy method, which would be more computationally efficient and less dependent on the calibration parameters. For example, this could include adaptation of the recent work of the authors on the multi-resolution particle modelling for a smoother transition of MD particles to continuum hydrodynamics as well as considering the particle feedback effect on the flow. Future work will also address effects of the computational domain size and the peptide concentration in water on the effective focusing of peptide diffusion by the velocity strain field as well as evaluate the importance of correction for diffusion computations in the current small periodic computational domain.

5 Acknowledgments

6 Reference

[1]   G. H. W. Sanders and A. Manz, "Chip-based microsystems for genomic and proteomic analysis," *TrAC - Trends Anal. Chem.*, vol. 19, no. 6, pp. 364–378, 2000.

[2]   S. H. DeWitt, "Microreactors for chemical synthesis," *Curr. Opin. Chem. Biol.*, vol. 3, no. 3, pp. 350–356, 1999.

[3]   Y. N. Xia and G. M. Whitesides, "Soft lithography," *Annu. Rev. Mater. Sci.*, vol. 37, no. 5, pp. 551–575, 1998.

[4]   J. Greener *et al.*, "Rapid, cost-efficient fabrication of microfluidic reactors in thermoplastic polymers by combining photolithography and hot embossing," *Lab Chip*, vol. 10, no. 4, pp. 522–524, 2010.

[5]   H. Song, D. L. Chen, and R. F. Ismagilov, "Reactions in droplets in microfluidic channels," *Angew. Chemie - Int. Ed.*, vol. 45, no. 44, pp. 7336–7356, 2006.

[6]   P. J. A. Kenis, R. F. Ismagilov, G. M. Whitesides, P. J. A. Kenis, R. F. Ismagilov, and G. M. Whitesides, "Microfabrication Inside Capillaries Using Multiphase Laminar Flow Patterning Published by : American Association for the Advancement of Science Stable URL : http://www.jstor.org/stable/2898259 Microfabrication Inside Capitlaries Using Muttiphase Laminar F," vol. 285, no. 5424, pp. 83–85, 2017.

[7]   P. J. A. Kenis, R. F. Ismagilov, S. Takayama, G. M. Whitesides, S. Li, and H. S. White, "Fabrication inside microchannels using fluid flow," *Acc. Chem. Res.*, vol. 33, no. 12, pp. 841–847, 2000.

[8]   P. K. Wong, Y. K. Lee, and C. M. Ho, "Deformation of DNA molecules by hydrodynamic focusing," *J. Fluid Mech.*, vol. 497, no. 497, pp. 55–65, 2003.

[9]   C. N. Baroud, F. Okkels, L. Ménétrier, and P. Tabeling, "Reaction-diffusion dynamics: Confrontation between theory and experiment in a microfluidic reactor," *Phys. Rev. E - Stat. Physics, Plasmas, Fluids, Relat. Interdiscip. Top.*, vol. 67, no. 6, p. 4, 2003.

[10]   G. Nair *et al.*, "In situ fabrication of cross-linked protein membranes by using microfluidics," *ChemBioChem*, vol. 7, no. 11, pp. 1683–1689, 2006.

[11]   B. H. Weigl, P. Yager, B. H. Weigl, and P. Yager, "Linked references are available on JSTOR for this article : Microfluidic Diffusion-Based Separation and Detection," vol. 283, no. 5400, pp. 346–347, 2016.

[12]   W. E. TeGrotenhuis, R. J. Cameron, V. V Viswanathan, and R. S. Wegeng, "Solvent Extraction and Gas Absorption Using Microchannel Contactors," in *Microreaction Technology: Industrial Prospects*, 2000, pp. 541–549.

[13]   W. E. TeGrotenhuis, R. J. Cameron, M. G. Butcher, P. M. Martin, and R. S. Wegeng, "Microchannel devices for efficient contacting of liquids in solvent extraction," *Sep. Sci. Technol.*, vol. 34, no. 6–7, pp. 951–974, 1999.

[14]   H. Hisamoto, T. Horiuchi, M. Tokeshi, A. Hibara, and T. Kitamori, "On-chip integration of neutral ionophore-based ion pair extraction reaction," *Anal. Chem.*, vol. 73, no. 6, pp. 1382–1386, 2001.

[15] A. J. Chorin, "A numerical method for solving incompressible viscous flow problems," *J. Comput. Phys.*, vol. 2, no. 1, pp. 12–26, 1967.

[16]   K. Ritos, M. K. Borg, D. A. Lockerby, D. R. Emerson, and J. M. Reese, "Hybrid molecular-continuum simulations of water flow through carbon nanotube membranes of realistic thickness," *Microfluid. Nanofluidics*, vol. 19, no. 5, pp. 997–1010, 2015.

[17]   S. T. O'Connell and P. A. Thompson, "Molecular dynamics-continuum hybrid computations: A tool for studying complex fluid flows," *Phys. Rev. E*, vol. 52, no. 6, pp. R5792--R5795, Dec. 1995.

[18]   X. B. Nie, S. Y. Chen, W. N. E, and M. O. Robbins, "A continuum and molecular dynamics hybrid method for micro- and nano-fluid flow," *J. Fluid Mech.*, vol. 500, pp. 55–64, 2004.

[19]   E. G. Flekkøy, G. Wagner, and J. Feder, "Hybrid model for combined particle and continuum dynamics," *Europhys. Lett.*, vol. 52, no. November, pp. 271–276, 2000.

[20]   N. Asproulis, M. Kalweit, and D. Drikakis, "A hybrid molecular continuum method using point wise coupling," *Adv. Eng. Softw.*, vol. 46, no. 1, pp. 85–92, 2012.

[21]   I. A. Cosden and J. R. Lukes, "A hybrid atomistic-continuum model for fluid flow using LAMMPS and OpenFOAM," *Comput. Phys. Commun.*, vol. 184, no. 8, pp. 1958–1965, 2013.

[22]   P. M. Kulkarni, C.-C. Fu, M. S. Shell, and L. Gary Leal, "Multiscale modeling with smoothed dissipative particle dynamics," *J. Chem. Phys.*, vol. 138, no. 23, p. 234105, 2013.

[23]   D. A. Fedosov and G. E. Karniadakis, "Triple-decker: Interfacing atomistic-mesoscopic-continuum flow regimes," *J. Comput. Phys.*, vol. 228, no. 4, pp. 1157–1171, 2009.

[24]   N. D. Petsev, L. Gary Leal, and M. Scott Shell, "Hybrid molecular-continuum simulations using smoothed dissipative particle dynamics," *J. Chem. Phys.*, vol. 142, no. 4, 2015.

[25]   M. Praprotnik, L. Delle Site, and K. Kremer, "Adaptive resolution molecular-dynamics simulation: Changing the degrees of freedom on the fly," *J. Chem. Phys.*, vol. 123, no. 22, 2005.

[26]   J. Zavadlav and M. Praprotnik, "Adaptive resolution simulations coupling atomistic water to dissipative particle dynamics," *J. Chem. Phys.*, vol. 147, no. 11, 2017.

[27]   R. Delgado-Buscalioni, J. Sablić, and M. Praprotnik, "Open boundary molecular dynamics," *Eur. Phys. J. Spec. Top.*, vol. 224, no. 12, pp. 2331–2349, 2015.

[28]   J. Sablić, M. Praprotnik, and R. Delgado-Buscalioni, "Open boundary molecular dynamics of sheared star-polymer melts," *Soft Matter*, vol. 12, no. 8, pp. 2416–2439, 2016.

[29] J. Sablić, M. Praprotnik, and R. Delgado-Buscalioni, "Deciphering the dynamics of star molecules in shear flow," *Soft Matter*, vol. 13, no. 29, pp. 4971–4987, 2017.

[30] J. Sablić, R. Delgado-Buscalioni, and M. Praprotnik, "Application of the Eckart frame to soft matter: Rotation of star polymers under shear flow," *Soft Matter*, vol. 13, no. 39, pp. 6988–7000, 2017.

[31] J. H. Walther, M. Praprotnik, E. M. Kotsalis, and P. Koumoutsakos, "Multiscale simulation of water flow past a C540fullerene," *J. Comput. Phys.*, vol. 231, no. 7, pp. 2677–2681, 2012.

[32] D. Elrick, "Source Functions for Diffusion in Uniform Shear Flow," *Aust. J. Phys.*, vol. 15, no. 3, p. 283, 1962.

[33] S. Hess and J. C. Rainwater, "Diffusion in a laminar flow: Shear rate dependence of correlation functions and of effective transport coefficients," *J. Chem. Phys.*, vol. 80, no. 3, p. 1295, 1984.

[34] D. J. Evans, W. G. Hoover, B. H. Failor, B. Moran, and A. J. C. Ladd, "Nonequilibrium molecular dynamics via Gauss's principle of least constraint," *Phys. Rev. A*, vol. 28, no. 2, pp. 1016–1021, Aug. 1983.

[35] D. J. Evans, "Thermal conductivity of the Lennard-Jones fluid," *Phys. Rev. A*, vol. 34, no. 2, pp. 1449–1453, 1986.

[36] S. H. Lee, D. K. Park, and D. B. Kang, "Molecular dynamics simulations for transport coefficients of liquid argon: new approaches," *Bull. Korean Chem. Soc.*, vol. 24, no. 2, pp. 178–182, 2003.

[37]   C. Braga, A. Galindo, and E. A. Müller, "Nonequilibrium molecular dynamics simulation of diffusion at the liquid-liquid interface," *J. Chem. Phys.*, vol. 141, no. 15, p. 154101, 2014.

[38]   A. Einstein, "On the Motion of Small Particles Suspended in a Stationary Liquid, as Required by the Molecular Kinetic Theory of Heat," *Ann. Phys.*, vol. 322, pp. 549–560, 1905.

[39]   R. Kubo, M. Toda, and N. Hashitsume, *Statistical Physics II*, 2nd ed. Berlin: Springer-Verlag, 1991.

[40]   M. S. Green, "Markoff Random Processes and the Statistical Mechanics of Time‐Dependent Phenomena," *J. Chem. Phys.*, vol. 20, no. 8, pp. 1281–1295, 1952.

[41]   M. P. Allen and D. J. Tildesley, *Computer Simulation of Liquids*. New York, NY, USA: Clarendon Press, 1989.

[42]   A. Markesteijn, S. Karabasov, A. Scukins, D. Nerukh, V. Glotov, and V. Goloviznin, "Concurrent multiscale modelling of atomistic and hydrodynamic processes in liquids," *Philos. Trans. R. Soc. A Math. Phys. Eng. Sci.*, vol. 372, no. 2021, pp. 20130379–20130379, 2014.

[43]   A. Scukins, D. Nerukh, E. Pavlov, S. Karabasov, and A. Markesteijn, "Multiscale molecular dynamics/hydrodynamics implementation of two dimensional 'Mercedes Benz' water model," *Eur. Phys. J. Spec. Top.*, vol. 224, no. 12, pp. 2217–2238, 2015.

[44]   E. Pavlov, M. Taiji, A. Scukins, A. Markesteijn, S. Karabasov, and D. Nerukh, "Visualising and controlling the flow in biomolecular systems at and between multiple scales: From atoms to hydrodynamics at different locations in time and space," *Faraday Discuss.*, vol. 169, pp. 285–302, 2014.

[45]   L. D. Landau and E. M. Lifshitz, *Statistical physics. Part 1*. Amsterdam; London: Elsevier Butterworth Heinemann, 1980.

[46]   I. Korotkin, S. Karabasov, D. Nerukh, A. Markesteijn, A. Scukins, and V. Farafonov, "A hybrid molecular dynamics/fluctuating hydrodynamics method for modelling liquids at multiple scales in space and time," *J. Chem. Phys.*, vol. 143, no. 1, 2015.

[47]   I. Korotkin, D. Nerukh, E. Tarasova, V. Farafonov, and S. Karabasov, "Two-phase flow analogy as an effective boundary condition for modelling liquids at atomistic resolution," *J. Comput. Sci.*, vol. 17, pp. 446–456, Nov. 2016.

[48]   E. Tarasova, I. Korotkin, V. Farafonov, S. Karabasov, and D. Nerukh, "Complete virus capsid at all-atom resolution: Simulations using molecular dynamics and hybrid molecular dynamics/hydrodynamics methods reveal semipermeable membrane function," *J. Mol. Liq.*, 2017.

[49]   M. J. Abraham *et al.*, "GROMACS: High performance molecular simulations through multi-level parallelism from laptops to supercomputers," *SoftwareX*, vol. 1–2, pp. 19–25, Sep. 2015.

[50]   D. Van Der Spoel, E. Lindahl, B. Hess, G. Groenhof, A. E. Mark, and H. J. C. Berendsen, "GROMACS: Fast, flexible, and free," *J. Comput. Chem.*, vol. 26, no. 16, pp. 1701–1718, Dec. 2005.

[51]   J. Hu, I. A. Korotkin, and S. A. Karabasov, "A multi-resolution particle/fluctuating hydrodynamics model for hybrid simulations of liquids based on the two-phase flow analogy," *J. Chem. Phys.*, vol. 149, no. 8, p. 084108, 2018.

[52] I. Korotkin and S. Karabasov, "A Generalised Landau-Lifshitz Fluctuating Hydrodynamics model for concurrent simulations of liquids at atomistic and continuum resolution," *J. Chem. Phys. Under Rev.*

[53] L. V. A. Breedveld, *Shear-Induced self-diffusion in concentrated suspensions*. 2000.

[54] W. C. Sandberg and D. M. Heyes, "Self-diffusion in equilibrium and sheared liquid mixtures by molecular dynamics," *Mol. Phys.*, vol. 85, no. 3, pp. 635–649, 1995.

[55] J. D. Moore, S. T. Cui, H. D. Cochran, and P. T. Cummings, "A molecular dynamics study of a short-chain polyethylene melt. I. Steady-state shear," *J. Nonnewton. Fluid Mech.*, vol. 93, no. 1, pp. 83–99, 2000.

[56] P. T. Cummings, B. Y. Wang, D. J. Evans, and K. J. Fraser, "Nonequilibrium molecular-dynamics calculation of self- diffusion in a non-newtonian fluid subject to a couette strain field," *J. Chem. Phys.*, vol. 94, no. 3, pp. 2149–2158, 1991.

[57] A. P. Markesteijn, S. A. Karabasov, V. Y. Glotov, and V. M. Goloviznin, "A new non-linear two-time-level Central Leapfrog scheme in staggered conservation–flux variables for fluctuating hydrodynamics equations with GPU implementation," *Comput. Methods Appl. Mech. Eng.*, vol. 281, pp. 29–53, Nov. 2014.

[58] L. Verlet, "Computer 'Experiments' on Classical Fluids. I. Thermodynamical Properties of Lennard-Jones Molecules," *Phys. Rev.*, vol. 159, no. 1, pp. 98–103, Jul. 1967.

[59] D. J. Evans and G. Morriss, *Statistical mechanics of nonequilibrium liquids, second edition*. 2008.

[60] B. D. Todd, "Computer simulation of simple and complex atomistic fluids by nonequilibrium molecular dynamics techniques," in *Computer Physics Communications*, 2001, vol. 142, no. 1–3, pp. 14–21.

[61] W. G. Hoover and C. G. Hoover, "Links between microscopic and macroscopic fluid mechanics," *Mol. Phys.*, vol. 101, no. 11, pp. 1559–1573, 2003.

[62] D. A. McQuarrie, *Statistical mechanics*. New York: Harper & Row, 1976.

[63] J. H. Wang, "Self-Diffusion Coefficients of Water," *J. Phys. Chem.*, vol. 69, no. 12, p. 4412, Dec. 1965.

[64] B. Dünweg and K. Kremer, "Molecular dynamics simulation of a polymer chain in solution," *J. Chem. Phys.*, vol. 99, no. 9, pp. 6983–6997, 1993.

[65] T. King, S. Butcher, and L. Zalewski, "Apocrita - High Performance Computing Cluster for Queen Mary University of London," Mar. 2017.

[66] H. J. C. Berendsen, D. van der Spoel, and R. van Drunen, "GROMACS: A message-passing parallel molecular dynamics implementation," *Comput. Phys. Commun.*, vol. 91, no. 1, pp. 43–56, 1995.